Progress in Fractional Differentiation and Applications
An International Journal

http://dx.doi.org/10.18576/pfda/110404

Two Weighted Average Finite Difference Schemes for Variable-Order Fractional Mixed Diffusion and Diffusion-Wave Equation

Nasser. H. Sweilam[1,*], *Adel.A. Darwish*[2], *Nada Henidy*[3], *and Salma A. Shatta*[2]

[1]Department of Mathematics, Faculty of Science, Cairo University, Giza, Egypt
[2]Department of Mathematics, Faculty of Science, Helwan University, Cairo, Egypt
[3]Department of Mathematics, Obour Higher Institute of Management, Computers and MIS, Cairo, Egypt

Received: 22 Feb. 2025, Revised: 23 Apr. 2025, Accepted: 23 Jun. 2025
Published online: 1 Oct. 2025

Abstract: In this paper is investigated variable-order mixed diffusion and diffusion-wave model problems. The variable-order derivatives are formulated using the Caputo definition. For the numerical computation of these equations in one and two dimensions, we propose two weighted average finite difference methods: a nonstandard and a standard approach. We further analyze the stability and truncation error of these schemes. Numerical experiments illustrate the memory properties of the proposed methods and establish their computational effectiveness and numerical accuracy. The results confirm that the proposed methods efficiently solve variable-order equations.

Keywords: Caputo derivative; mixed diffusion and diffusion-wave model problem, nonstandard and standard weighted average finite difference methods, stability analysis

1 Introduction

In recent years, the applications of partial differential equations (PDEs) were more accurately and effectively represented through the use of fractional-order derivatives. These fractional derivative operators expanded the traditional concept of differentiation to non-integer orders and were widely used in PDEs. Fractional partial differential equations (FPDEs) involving constant-order derivatives found widespread application in modeling diffusion processes [1]-[9]. Recently, researchers have turned their attention toward variable-order derivatives, in which the derivative order depends on space and/or time. This extension offers a more accurate representation of systems exhibiting spatially or temporally varying memory effects [10]-[24]. The variable order of PDEs (VOPDEs) is widely applied in biology, engineering, and finance. They are particularly useful for modeling complex phenomena such as sub-diffusion equations with the coefficients that are functions of spatial variables [10] and non-autonomous time-fractional diffusion equations involving a variable order depending on space [11]. Numerical methods for VOPDEs have seen significant advancements. For instance, Wang et al. [15] established a discretization approach for variable-order diffusion-wave equations, where the derivative order depends on space and/or time. Also, they combined Grünwald-Letnikov operators with Bernoulli polynomials to achieve accurate second-order convergence. Shen et al. [19] proposed a stable characteristic finite difference method for variable-order fractional advection-diffusion equations with nonlinear source terms, demonstrating improved computational performance. Moreover, the mixed diffusion and diffusion-wave equation with time-fractional derivatives has been extensively studied [6], [7]. This equation incorporates both fractional diffusion and diffusion-wave terms, where the fractional order lies within the ranges $(0,1)$ and $(1,2)$, respectively. To efficiently solve this equation, Sun et al. [6] developed a finite difference method based on the L_1 approach. The present study investigates the extending of classical mixed diffusion and diffusion-wave models [6], [7] to variable-order mixed diffusion and diffusion-wave model problems (VOMDW). Specifically, variable-order calculus extends constant-order theories, whether integer or

* Corresponding author e-mail: nsweilam@sci.cu.edu.eg

non-integer. With the order is formulated relative to quantities such as spatial variables, time measurements, and more [13]-[23]. The following variable-order mixed diffusion and diffusion-wave model problems in two dimensions (2-D) are formulated using Caputo derivatives:

$$ {}_0^cD_t^{\nu(x,y,t)}\,u(x,y,t)+{}_0^cD_t^{\gamma(x,y,t)}\,u(x,y,t)=\Delta u(x,y,t)+f(x,y,t). \tag{1}$$

The initial conditions for this equation are:

$$u(x,y,t_0)=v_1(x,y,t_0),\quad \frac{\partial u(x,y,t_0)}{\partial t}=v_2(x,y,t_0),\quad (x,y)\in\Omega,$$

and the boundary conditions are:

$$\begin{aligned} &u(X_0,y,t)=h_1(X_0,y,t),\quad u(X,y,t)=h_2(X,y,t),\\ &u(x,Y_0,t)=h_3(x,Y_0,t),\quad u(x,Y,t)=h_4(x,Y,t),\quad t\in[0,T_f]. \end{aligned}$$

Since $0<\nu(x,y,t)\le 1$, $1<\gamma(x,y,t)\le 2$ and $T_f>0$. The functions f, v_1,v_2 and h_i, for $i\in\{1,2,3,4\}$ are considered known and sufficiently regular over the closed, convex, and bounded domain Ω.
The main benefit of variable-order partial differential equations (VOPDEs) is their ability to capture power-law behaviors and memory effects that are commonly observed in complex systems, which ordinary integer-order derivatives fail to represent [2]. However, traditional numerical methods require modifications to accommodate the Caputo fractional nature of the derivatives, necessitating adjustments to finite difference and nonstandard finite difference techniques. Furthermore, the inclusion of non-integer order derivatives may lead to less regular solutions, influencing numerical schemes, stability, and convergence characteristics. The primary objective of this work is formulating numerical schemes that solve VOMDW model problems. Specifically, we analyze and compare two numerical methods: the weighted average standard finite difference method (WASFDM) and the weighted average nonstandard finite difference method (WANSFDM). The WASFDM employs a weighted factor [4,5], while the WANSFDM is proposed to enhance solution accuracy. The paper is structured as described below: The definitions and fundamental concepts are presented in Section 2. Section 3 details the construction of the WANSFDM and analyzes its stability. In Section 4, we evaluate the proposed methods numerically, with final conclusions given in Section 5.

2 Fundamental Concepts and Notations

2.1 Some Definitions

This section introduces several definitions related to the variable-order derivatives. The definitions presented here extend the concepts introduced in references [4,5].

Definition 2.1. The variable-order Riemann-Liouville derivatives for $t\in(a,b)$, both right-sided and left-sided, follow as:

$$\begin{aligned} {}^{RL}D_{b^-}^{\nu(x,y,t)}\,u(t) &= {}^{RL}D_{t,b}^{\nu(x,y,t)}\,u(t)\\ &= \frac{d^n}{dt^n}\frac{(-1)^n}{\Gamma(n-\nu(x,y,t))}\int_t^b \frac{u(s)}{(s-t)^{1-n+\nu(x,y,t)}}\,ds,\quad t<b,\\ {}^{RL}D_{a^+}^{\nu(x,y,t)}\,u(t) &= {}^{RL}D_{a,t}^{\nu(x,y,t)}\,u(t)\\ &= \frac{d^n}{dt^n}\frac{1}{\Gamma(n-\nu(x,y,t))}\int_a^t \frac{u(s)}{(t-s)^{1-n+\nu(x,y,t)}}\,ds,\quad t>a, \end{aligned}$$

where $n-1\le\nu(x,y,t)<n$ is the variable-order, n is a positive integer and $\Gamma(\cdot)$ is the Gamma function.

Definition 2.2. The variable-order Caputo derivatives for $t \in (a,b)$, both right-sided and left-sided are defined as follows:

$$
\begin{aligned}
{}^{C}D_{b^-}^{\nu(x,y,t)}\,u(t) &= {}^{C}D_{t,b}^{\nu(x,y,t)}\,u(t) \\
&= \frac{1}{\Gamma(n-\nu(x,y,t))}\int_t^b \frac{u^{(n)}(s)}{(s-t)^{1-n+\nu(x,y,t)}}\,ds, \quad t<b, \\
{}^{C}D_{a^+}^{\nu(x,y,t)}\,u(t) &= {}^{C}D_{a,t}^{\nu(x,y,t)}\,u(t) \\
&= \frac{1}{\Gamma(n-\nu(x,y,t))}\int_a^t \frac{u^{(n)}(s)}{(t-s)^{1-n+\nu(x,y,t)}}\,ds, \quad t>a,
\end{aligned}
$$

where $n-1 \le \nu(x,y,t) < n$ is the variable-order, n is a positive integer and $\Gamma(\cdot)$ is the Gamma function.

Definition 2.3. The right-sided and left-sided variable-order Grünwald-Letnikov derivatives of $u(t)$ are respectively defined as:

$$
{}^{GL}D_{t,b}^{\nu(x,y,t)}\,u(t) = \lim_{r\to 0} r^{-\nu(x,y,t)}\left[\sum_{j=0}^{\lfloor \frac{t}{r} \rfloor} w_j^{\nu(x,y,t)} u(t+jr)\right],
$$

$$
{}^{GL}D_{a,t}^{\nu(x,y,t)}\,u(t) = \lim_{r\to 0} r^{-\nu(x,y,t)}\left[\sum_{j=0}^{\lfloor \frac{t}{r} \rfloor} w_j^{\nu(x,y,t)} u(t-jr)\right].
$$

where $w_j^{\nu(x,y,t)}$ are the normalized Grünwald's weights defined by $w_j^{\nu(x,y,t)} = (-1)^j \binom{\nu(x,y,t)}{j}$, and $\lfloor t/r \rfloor$ denotes the largest integer k such that $k \cdot r \le t$ at $\nu(x,y,t) > 0$, $t \in (a,b)$.

2.2 NSFDM discretization

A scheme qualifies as a nonstandard finite difference method (NSFDM) if either condition holds [27]:
1. Uses nonlocal approximations for PDE terms.
2. Employs nontraditional discretization with positive function $\kappa(h) = h + O(h^2), 0 < \kappa < 1, \forall h > 0$, where $\kappa(h)$ is a continuous function.

3 WANSFDM for VOFMDW

We apply a weighted average finite difference scheme based on a designated weight factor to approximate variable-order derivatives. The two-dimensional spatial domain is discretized as follows:

$t_k = k\,\Delta t,\ x_i = i\,\Delta x,\ y_j = j\,\Delta y,$ with indices $k = 0:\ell,\ i = 0:m,\ j = 0:n.$

Considering that $\ell, m, n \in \mathbb{N}$ are natural numbers representing the number of divisions in time and the spatial grids along the x and $y-$coordinates, respectively, the parameters Δt, Δx and Δy correspond to the time and spatial step sizes and are defined by:

$$
\Delta t = \frac{t_k - t_0}{\ell}, \quad \Delta x = \frac{x_i - x_0}{m}, \quad \text{and} \quad \Delta y = \frac{y_j - y_0}{n}.
$$

Using a weighted average finite difference approximation, we discretize the solution as:

$$
u_{i,j}^k = u(x_0 + i\Delta x, y_0 + j\Delta y, t_0 + k\Delta t).
$$

Then, WANSFDM can be formulated as:

$$
u_{i,j}^k \approx (1-\beta)\,u_{i,j}^{k+1} + \beta\,u_{i,j}^k, \quad 0 \le \beta \le 1.
$$

3.1 *Numerical discretization of* WANSFDM *using Caputo derivatives*

The discretized form of the VOMDW model problems 1, using definition (2), is given as follows:

$$
\begin{aligned}
&H_1 \textstyle\sum_{k=0}^{n} w_k^{\nu}(u_{i,j}^{n-k+1} - u_{i,j}^{n-k}) + H_2 \textstyle\sum_{k=0}^{n} w_k^{\gamma}(u_{i,j}^{n-k+1} - 2u_{i,j}^{n-k} + u_{i,j}^{n-k-1}) - \\
&(1-\beta)\ \bigtriangledown^2 u^{k+1} - \beta\ \bigtriangledown^2 u^k = R_{i,j}^k,
\end{aligned} \tag{2}
$$

where

$$\bigtriangledown^2 u^k = \frac{u^k_{i+1,j} - 2u^k_{i,j} + u^k_{i-1,j}}{(\kappa(\Delta x))^2} + \frac{u^k_{i,j+1} - 2u^k_{i,j} + u^k_{i,j-1}}{(\kappa(\Delta y))^2},$$

$$\bigtriangledown^2 u^{k+1} = \frac{u^{k+1}_{i+1,j} - 2u^{k+1}_{i,j} + u^{k+1}_{i-1,j}}{(\kappa(\Delta x))^2} + \frac{u^{k+1}_{i,j+1} - 2u^{k+1}_{i,j} + u^{k+1}_{i,j-1}}{(\kappa(\Delta y))^2},$$

and

$$H_1 = \frac{(\triangle t)^{1-\nu(x,y,t)}}{\tau(\triangle t)\ \Gamma(2-\nu(x,y,t))},\ \ w^\nu_k = (k+1)^{1-\nu(x,y,t)} - k^{1-\nu(x,y,t)},$$

$$H_2 = \frac{(\triangle t)^{2-\gamma(x,y,t)}}{(\tau(\triangle t))^2\ \Gamma(3-\gamma(x,y,t))},\ \ w^\gamma_k = (k+1)^{2-\gamma(x,y,t)} - k^{2-\gamma(x,y,t)},$$

and $R^k_{i,j}$ represents the truncation error. Neglecting this error, the resulting computational finite difference scheme is formulated as follows:

$$\begin{aligned} &H_1 \textstyle\sum_{k=0}^n w^\nu_k (u^{n-k+1}_{i,j} - u^{n-k}_{i,j}) + H_2 \sum_{k=0}^n w^\gamma_k (u^{n-k+1}_{i,j} - 2u^{n-k}_{i,j} + u^{n-k-1}_{i,j}) - \\ &(1-\beta)\ \bigtriangledown^2 u^{k+1} - \beta\ \bigtriangledown^2 u^k = 0, \end{aligned} \tag{3}$$

3.2 *Stability and convergence of* WANSFDM

To analyze the stability of WANSFDM, we apply a modified von Neumann stability analysis [24]. Assuming a Fourier mode solution: $u^n_{i,j} = G^n e^{I(ik_x\Delta x + jk_y\Delta y)}$, where G is the amplification factor, the propagation in the x and $y-$coordinates is characterized by the wave numbers K_x, K_y and $I = \sqrt{-1}$. By substituting this assumption into equation 3 and utilizing Euler's formula, $e^{I\rho} = cos(\rho) + Isin(\rho)$, we obtain:

$$\begin{aligned} &G\left[H_1 \textstyle\sum_{k=0}^n w^\nu_k G^{-k} + H_2 \sum_{k=0}^n w^\gamma_k G^{-k} + \mathscr{L}(\beta-1)\right] - H_1 \sum_{k=0}^n w^\nu_k G^{-k} - \\ &2H_2 \textstyle\sum_{k=0}^n w^\gamma_k G^{-k} - \mathscr{L}\beta + H_2 \sum_{k=0}^n w^\gamma_k G^{-k-1} = 0, \end{aligned} \tag{4}$$

where $\mathscr{L}$ represents the spatial discretization terms:

$$\mathscr{L} = 2\left[\frac{cos(k_x\Delta x) - 1}{(\kappa(\Delta x))^2} + \frac{cos(k_y\Delta y) - 1}{(\kappa(\Delta y))^2}\right].$$

The scheme will be stable when $|G| \le 1$. Multiplying by G in equation 4, we obtain the characteristic equation:

$$\begin{aligned} &G^2[H_1 \textstyle\sum_{k=0}^n w^\nu_k G^{-k} + H_2 \sum_{k=0}^n w^\gamma_k G^{-k} + \mathscr{L}(\beta-1)] - G[H_1 \sum_{k=0}^n w^\nu_k G^{-k} + \\ &2H_2 \textstyle\sum_{k=0}^n w^\gamma_k G^{-k} + \mathscr{L}\beta] + H_2 \sum_{k=0}^n w^\gamma_k G^{-k} = 0, \end{aligned} \tag{5}$$

which simplifies to:

$$G^2[A + B + \mathscr{L}(\beta-1)] - G[A + 2B + \mathscr{L}\beta] + B = 0, \tag{6}$$

where

$$A = H_1 \sum_{k=0}^n w^\nu_k G^{-k},\ \ B = H_2 \sum_{k=0}^n w^\gamma_k G^{-k}.$$

The stability condition requires:

$$|G_1| = \frac{|A + 2B + \mathscr{L}\beta + \sqrt{(A + 2B + \mathscr{L}\beta)^2 - 4(A + B + \mathscr{L}(\beta-1))B}|}{|2(A + H_2B + \mathscr{L}(\beta-1))|} \le 1,$$

which simplifies to:

$$|A + 2B + \mathscr{L}\beta + \sqrt{(A + 2B + \mathscr{L}\beta)^2 - 4(A + B + \mathscr{L}(\beta-1))B}| \le |2(A + B + \mathscr{L}(\beta-1))|.$$

Similarly, for G_2 :

$$|G_2| = \frac{|A+2B+\mathscr{L}\beta - \sqrt{(A+2B+\mathscr{L}\beta)^2 - 4(A+B+\mathscr{L}(\beta-1))B}|}{|2(A+H_2B+\mathscr{L}(\beta-1))|} \leq 1,$$

which simplifies to:

$$|A+2B+\mathscr{L}\beta - \sqrt{(A+2B+\mathscr{L}\beta)^2 - 4(A+B+\mathscr{L}(\beta-1))B}| \leq |2(A+B+\mathscr{L}(\beta-1))|.$$

Thus, if these inequalities are satisfied, the stability condition holds for all Fourier modes.

3.3 *Truncation error analysis*

Theorem 3.1. The truncation error of WANSFDM is given as follows, [25], [24]:

$$R_{i,j}^k = O((\frac{1}{2}-\beta)\triangle t + \frac{1}{6}(\triangle t)^2 - \frac{1}{12}(\Delta x)^2 - \frac{1}{12}(\Delta y)^2),$$

proof By referring to the truncation error definition in (2) and employing the Taylor series expansion with respect to time, we establish the following:

$$u_{i,j}^{n-k+1} = u(x_i,y_j,t_{n-k}+\tau(\Delta t)) = u_{i,j}^{n-k} + \tau(\Delta t)(\frac{\partial u}{\partial t})_{i,j}^{n-k} + \frac{1}{2}(\tau(\Delta t))^2(\frac{\partial^2 u}{\partial t^2})_{i,j}^{n-k} + \frac{1}{6}(\tau(\Delta t))^3(\frac{\partial^3 u}{\partial t^3})_{i,j}^{n-k} + \dots,$$

$$u_{i,j}^{k+1} = u(x_i,y_j,t_k+\tau(\Delta t)) = u_{i,j}^{k} + \tau(\Delta t)(\frac{\partial u}{\partial t})_{i,j}^{k} + \frac{1}{2}(\tau(\Delta t))^2(\frac{\partial^2 u}{\partial t^2})_{i,j}^{k} + \frac{1}{6}(\tau(\Delta t))^3(\frac{\partial^3 u}{\partial t^3})_{i,j}^{k} + \dots,$$

$$u_{i,j}^{k-1} = u(x_i,y_j,t_k-\tau(\Delta t)) = u_{i,j}^{k} - \tau(\Delta t)(\frac{\partial u}{\partial t})_{i,j}^{k} + \frac{1}{2}(\tau(\Delta t))^2(\frac{\partial^2 u}{\partial t^2})_{i,j}^{k} - \frac{1}{6}(\tau(\Delta t))^3(\frac{\partial^3 u}{\partial t^3})_{i,j}^{k} + \dots.$$

Likewise, we derive the equation for the spatial variable and substitute it into (2) for the 2D case, obtaining:

$${}^{C}D_t^{\nu(x,y,t)}u(x,y,t) = \frac{(\triangle t)^{1-\nu(x,y,t)}}{\Gamma(2-\nu(x,y,t))}\sum_{k=0}^{n} w_k^{\nu}((\frac{\partial u}{\partial t})_{i,j,n-k} + \frac{1}{2}(\tau(\Delta t))(\frac{\partial^2 u}{\partial t^2})_{i,j,n-k} + \dots)\delta_{n,k},$$

$${}^{C}D_t^{\gamma(x,y,t)}u(x,y,t) = \frac{(\triangle t)^{2-\gamma(x,y,t)}}{\Gamma(3-\gamma(x,y,t))}\sum_{k=0}^{n} w_k^{\gamma}((\frac{\partial^2 u}{\partial t^2})_{i,j,n-k} + \frac{1}{6}(\tau(\Delta t))^2(\frac{\partial^4 u}{\partial t^4})_{i,j,n-k} + \dots)\delta_{n,k},$$

$$\begin{aligned}(u_{xx})_{i,j}^k = &((1-\beta)((\frac{\partial^2 u}{\partial x^2})_{i,j,k+1} + \frac{1}{12}(\kappa(\Delta x))^2(\frac{\partial^4 u}{\partial x^4})_{i,j,k+1} + \dots)\\ &+\beta((\frac{\partial^2 u}{\partial x^2})_{i,j,k} + \frac{1}{12}(\kappa(\Delta x))^2(\frac{\partial^4 u}{\partial x^4})_{i,j,k} + \dots),\end{aligned} \tag{7}$$

$$\begin{aligned}(u_{yy})_{i,j}^k = &((1-\beta)((\frac{\partial^2 u}{\partial y^2})_{i,j,k+1} + \frac{1}{12}(\kappa(\Delta y))^2(\frac{\partial^4 u}{\partial y^4})_{i,j,k+1} + \dots)\\ &+\beta((\frac{\partial^2 u}{\partial y^2})_{i,j,k} + \frac{1}{12}(\kappa(\Delta y))^2(\frac{\partial^4 u}{\partial y^4})_{i,j,k} + \dots).\end{aligned} \tag{8}$$

Inserting these expressions (7), (8) into (2), we claim that a general value of β, the WANSFDM exhibits a local truncation error:

$$R_{i,j}^k = O((\frac{1}{2}-\beta)\tau(\triangle t) + \frac{1}{6}(\tau(\triangle t))^2 - \frac{1}{12}(\kappa(\Delta x))^2 - \frac{1}{12}(\kappa(\Delta y))^2, (\kappa(\Delta x))^4, (\kappa(\Delta y))^4, (\tau(\triangle t))^2),$$

but $\tau(\Delta t) = \Delta t + O(\Delta t^2)$, and $\kappa(h) = h + O(h^2)$, so

$$R_{i,j}^k = O((\frac{1}{2}-\beta)\triangle t + \frac{1}{6}(\triangle t)^2 - \frac{1}{12}(\Delta x)^2 - \frac{1}{12}(\Delta y)^2). \tag{9}$$

We can derive the truncation error of the 1-D VOFMDW equation using the same technique, Consequently, the WANSFDM's local truncation error is given as follows:

$$R_{i,j}^{k} = O((\frac{1}{2} - \beta)\triangle t + \frac{1}{6}(\triangle t)^2 - \frac{1}{12}(\Delta x)^2). \tag{10}$$

We observe that scheme (3) is explicit for $\beta = 1$ and implicit for $\beta = 0$. In particular, when β is chosen as $1/2$, it yields the Crank-Nicolson scheme. However, for the 1-D VOFMDW equation, if $0 < \beta < 1$ is chosen according to:

$$\beta = \frac{1}{2} + \frac{\triangle t}{6} - \frac{(\Delta x)^2}{12\triangle t}, \tag{11}$$

furthermore, the two-dimensional VOFMDW equation, in the form of

$$\beta = \frac{1}{2} + \frac{\triangle t}{6} - \frac{(\Delta x)^2}{12\triangle t} - \frac{(\Delta y)^2}{12\triangle t}. \tag{12}$$

4 Applications of WANSFDM and WASFDM

This section evaluates the computational efficiency and numerical accuracy of the developed numerical approaches for three test problems. All computations were conducted using MATLAB. The maximum error E_∞ is computed to assess the accuracy of the proposed schemes as follows:

$$E_\infty = \max_{i,j,k} \left| u_{\text{exact}} - u_{\text{app}} \right|, \tag{13}$$

where u_{exact} refers to the exact solution for the given test problems, while u_{app} denotes the computed approximate solution. They evaluated all spatial grid points (x_i, y_j) and time points t_k. Table 1 presents the stability analysis results for WANSFDM and WASFDM using different values of β. The analysis is conducted under fixed discretization parameters ($\ell = m = n = 15$), with coefficients $K_x = K_y = \pi$ and spatial domain ($X = Y = 1$). We examine three dominant cases of variable-order diffusion-wave dynamics, classified based on the relative values of the variable-orders ν and γ: (a) Diffusion-dominated case: when the order ν is relatively large (e.g., $\nu \approx 0.9$) and γ is smaller (e.g., $\gamma \approx 1.3$), the system tends to a diffusion equation.

(b) Balanced-dominated case: when both ν and γ take moderate values (e.g., $\nu \approx 0.7$, $\gamma \approx 1.7$), the model captures a balance between diffusion and wave propagation effects.

(c) Wave-dominated case: when ν is small (e.g., $\nu \approx 0.3$) and γ is large (e.g., $\gamma \approx 1.9$), the system tends to a wave equation. For short final times ($T_f = 1$), all schemes remain stable across all cases and values of β. However, as T_f increases, WANSFDM consistently demonstrates enhanced numerical stability compared to WASFDM, particularly in the diffusion-dominated and balanced cases. In the wave-dominated case, the instability of WASFDM becomes evident at larger values of T_f, especially for $\beta = 1$ and $\beta \in (0.5, 1]$ in as defined in Eq. (12). Using $\beta = 0.5$ or $\beta \in [0, 0.5]$ in Eq. (12) further improves WANSFDM stability compared to the standard scheme. Overall, the results indicate that WANSFDM offers improved performance in maintaining numerical stability over extended simulation times, particularly in scenarios governed by variable-order dynamics.

Table 1: The stability analysis of WANSFDM and WASFDM for $\ell = m = n = 15$, and $X = Y = 1$. Where S denotes a stable scheme and U corresponds to an unstable.

T_f	($\beta = 0$)		($\beta = 1$)		($\beta = 0.5$)		(β in Eq. (12))	
	WANSFDM	WASFDM	WANSFDM	WASFDM	WANSFDM	WASFDM	WANSFDM	WASFDM
Diffusion-dominated case $\nu \approx 0.9$, $\gamma \approx 1.3$								
1	S	S	S	S	S	S	S	S
15	S	S	S	S	S	S	S	S
20	S	U	S	U	S	U	S	S
Balanced-dominated case $\nu \approx 0.7$, $\gamma \approx 1.7$								
1	S	S	S	S	S	S	S	S
15	S	S	S	U	S	S	S	S
20	S	U	U	U	S	U	U	U
Wave-dominated case $\nu \approx 0.3$, $\gamma \approx 1.9$								
1	S	S	S	S	S	S	S	S
15	S	S	U	U	S	S	S	S
20	S	U	U	U	S	U	U	U

Problem 1

Consider the VOFMDW model described in [1], represented by the following equation:

$$f(x,t) = [\frac{t^{3+\gamma(x,t)}}{\Gamma(2-\nu(x,t))} + \frac{2+\nu(x,t)+\gamma(x,t)}{\Gamma(3-\gamma(x,t))} t^{3+\nu(x,t)}](3+\nu(x,t)+\gamma(x,t))e^{-x^2} + (2-4x^2)\, t^{3+\nu(x,t)+\gamma(x,t)} e^{-x^2}.$$

in which $t \in [0, T_f]$ and $x \in [0, X]$,
the initial conditions are:

$$u(x,0) = 0, \ \frac{\partial u(x,0)}{\partial t} = 0,$$

the corresponding boundary conditions are:

$$u(0,t) = t^{3+\nu(x,t)+\gamma(x,t)}, \ u(X,t) = t^{3+\nu(x,t)+\gamma(x,t)} e^{-X^2}.$$

For these given conditions, the exact solution is: $u(x,t) = t^{3+\nu(x,t)+\gamma(x,t)} e^{-x^2}$.
Considering the step sizes $\tau(\triangle t) = p \sinh(\triangle t)$ and $\kappa(\triangle x) = q(e^{\triangle x} - 1)$ for which $p, q \in (0,1)$, we compute the maximum error for Problem 1 is computed at various values of β, as shown in Table 2. The performance of WANSFDM and WASFDM depends significantly on the values of β and T_f. When $\beta = 0$ and $\beta = 0.5$, corresponding to the implicit and Crank-Nicholson schemes, respectively, WANSFDM exhibits higher accuracy for larger T_f. Therefore, WANSFDM is recommended for long-term simulations when $\beta = 0$ or $\beta = 0.5$ than the explicit scheme ($\beta = 1$). As T_f increases, errors also escalate, underscoring the critical role of selecting a proper scheme according to β and the simulation duration. Figure **??**, compares the exact and approximate solutions for u evaluated across the domain $x \in [0,1]$ for three distinct cases of ν and γ: (1) constant-order $\nu_0 = 0.9$, $\gamma_0 = 1.9$ (2) variable-order in linear functions $\nu(t) = 0.9 - 0.01\, t$, $\gamma(t) = 1.9 - 0.01\, t$ and (3) variable-order in nonlinear functions $\nu(x,t) = 0.9 - 0.01\, x^2\, t$, $\gamma(x,t) = 1.9 - 0.01\, x\, sin(t)$. The numerical simulations confirm that the approximate solution using the Caputo definition exhibits improved convergence toward the exact solution.

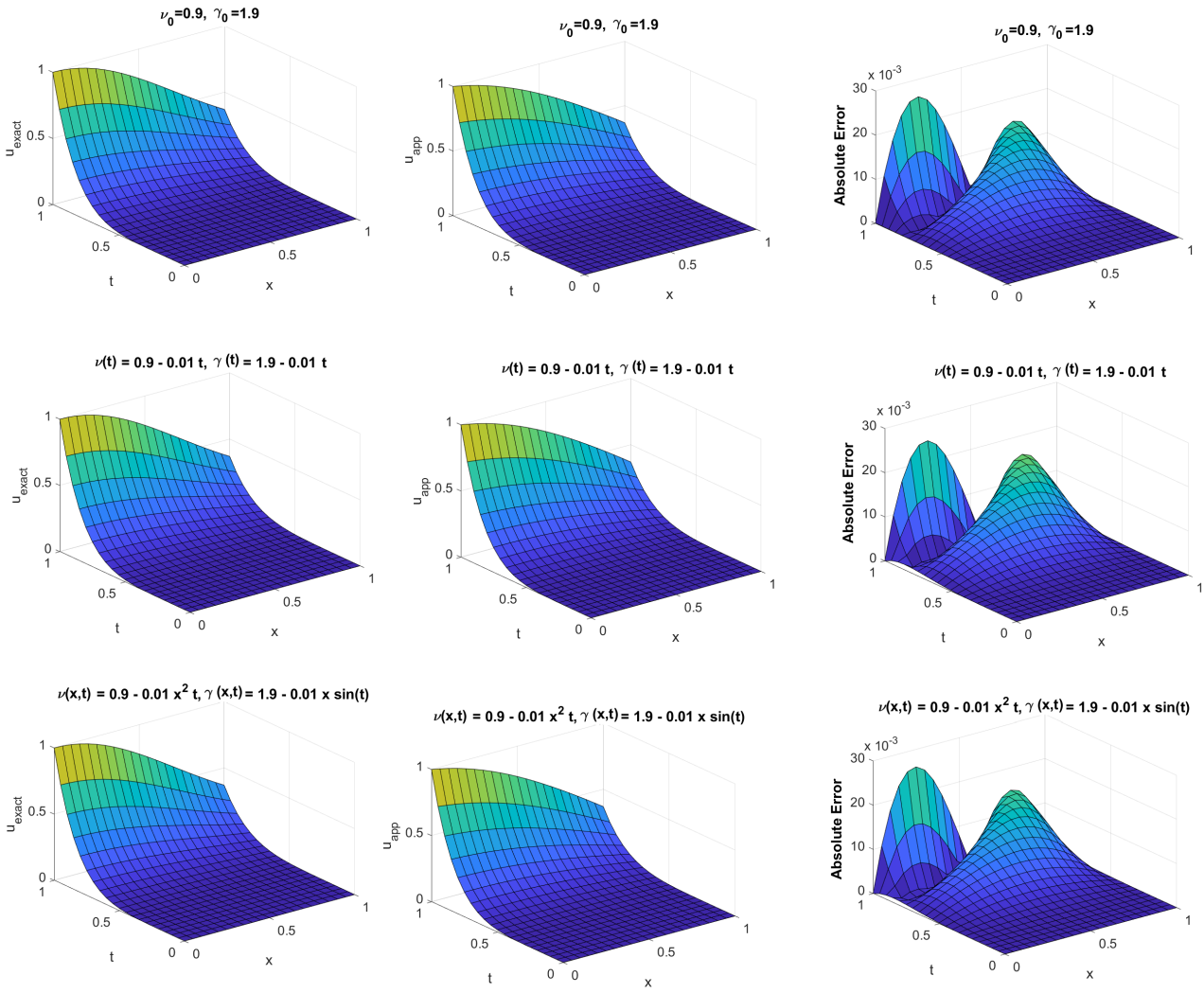

Figure 1. A comparison of three cases of exact and approximate solution behavior in Problem 1 when $n = m = 20$, with varying cases ν, γ, and $(x,t) \in [0,1] \times [0,1]$.

Table 2: The E_∞ error of WANSFDM and WASFDM for $n = m = 20$, $\nu(x,t) = 0.9 - 0.01\,t$, $\gamma(x,t) = 1.9 - 0.01\,t$, and $X = 1$.

T_f	$(\beta = 0)$		$(\beta = 1)$		$(\beta = 0.5)$	
	WANSFDM	WASFDM	WANSFDM	WASFDM	WANSFDM	WASFDM
0.1	3.844×10^{-7}	3.302×10^{-7}	2.407×10^{-7}	3.79×10^{-7}	2.008×10^{-7}	2.022×10^{-7}
0.2	2.996×10^{-5}	2.13×10^{-5}	7.512×10^{-6}	1.864×10^{-5}	1.906×10^{-5}	1.171×10^{-5}
0.35	5.407×10^{-4}	1.03×10^{-3}	4.474×10^{-4}	3.897×10^{-4}	3.891×10^{-4}	7.865×10^{-4}
0.6	4.718×10^{-3}	2.504×10^{-2}	2.588×10^{-2}	8.932×10^{-3}	3.205×10^{-3}	1.714×10^{-2}
1	2.369×10^{-2}	4.204×10^{-1}	7.015×10^{-1}	1.808×10^{-1}	3.448×10^{-2}	2.999×10^{-2}

Problem 2: Following [1], the 2-D VOFMDW as:

$$f(x,t) = [3t^2 + 6t + \frac{4}{C}t^3 + \frac{t^3}{C^2}((2x-1)^2 + (2y-1)^2)]exp(-\frac{(2x-1)^2}{4C} - \frac{(2y-1)^2}{4C}),$$

in which $t \in [0, T_f]$ and $\Omega \in [X_0, X] \times [Y_0, Y]$.
The initial conditions are:

$$u(x,y,0) = 0, \ \frac{\partial u(x,y,0)}{\partial t} = 0,$$

the corresponding boundary conditions are:

$$u(X_0,y,t) = t^3 exp(-\frac{(2X_0-1)^2}{4C} - \frac{(2y-1)^2}{4C}), \ u(X,y,t) = t^3 exp(-\frac{(2X-1)^2}{4C} - \frac{(2y-1)^2}{4C}),$$

$$u(x,Y_0,t) = t^3 exp(-\frac{(2x-1)^2}{4C} - \frac{(2Y_0-1)^2}{4C}), \ u(x,Y,t) = t^3 exp(-\frac{(2x-1)^2}{4C} - \frac{(Y-1)^2}{4C}).$$

For these given conditions, the exact solution is: $u(x,y,t) = t^3 exp(-\frac{(2x-1)^2}{4C} - \frac{(2y-1)^2}{4C})$.
For numerical approximation, we consider step sizes as $\tau(\triangle t) = p(e^{\triangle t} - 1)$, $\kappa(\triangle x) = q\,(e^{\triangle x} - 1)$ and $\kappa(\triangle y) = q\,(e^{\triangle y} - 1)$ for which $p, q \in (0,1)$. Figure **??**, compares the approximate numerical solutions for u, with the exact solution at $C = 0.05$, computed over the domain $(\Omega, t) \in [0,1]^2 \times [0, 0.1]$ for three distinct cases ν and γ: (1) constant-order $\nu_0 = 0.8$, $\gamma_0 = 1.7$ (2) variable-order in linear functions $\nu(t) = 0.8 - 0.01\,t$, $\gamma(t) = 1.7 - 0.01\,t$ and (3) variable-order in nonlinear functions $\nu(x,y,t) = 0.8 - 0.01\,t\,\cos(x\,y)$, $\gamma(x,y,t) = 1.7 - 0.01\,t\,\cos(x\,y)$, where the maximum error is minimized compared to the other two cases. For Problem 2, we evaluate the maximum error across various values of (X, Y, T_f), considering time-dependent variable-orders $\nu(t) = 0.7 - 0.01\,t$ and $\gamma(t) = 1.6 - 0.01\,t$, as shown in Table 3. Across all test cases, WANSFDM consistently demonstrates higher accuracy and improved numerical stability compared to WASFDM. Two configurations of the weighting parameter β are tested: the implicit case ($\beta = 0$) and the adaptive form defined in Eq. (12). Even when β in Eq. (12) varies with domain size, WANSFDM maintains consistent solution behavior and achieves maximum errors comparable to those of the implicit scheme. In contrast, WASFDM becomes unstable as the domain size increases, whereas WANSFDM remains robust to β variations.

Table 3: The E_∞ error of WANSFDM and WASFDM for $\ell = m = n = 15$, $\nu(t) = 0.7 - 0.01\,t$ and $\gamma(t) = 1.6 - 0.01\,t$.

(X,Y,T_f)	($\beta = 0$)		β in Eq. (12)	
	WANSFDM	WASFDM	WANSFDM	WASFDM
(0.1,0.1,0.1)	1.003×10^{-11}	2.471×10^{-11}	9.907×10^{-12}	2.553×10^{-11}
(0.1,0.1,0.2)	8.694×10^{-11}	2.004×10^{-10}	8.627×10^{-11}	2.0018×10^{-10}
(0.2,0.2,0.1)	9.978×10^{-9}	2.876×10^{-8}	9.8134×10^{-9}	2.852×10^{-8}
(2,2,0.1)	7.127×10^{-4}	1.993×10^{-3}	7.128×10^{-4}	1.978×10^{-3}
(1,1,1)	6.885×10^{-1}	2.721	6.892×10^{-1}	2.646
(1,2,1)	6.862×10^{-1}	2.833	6.870×10^{-1}	2.746

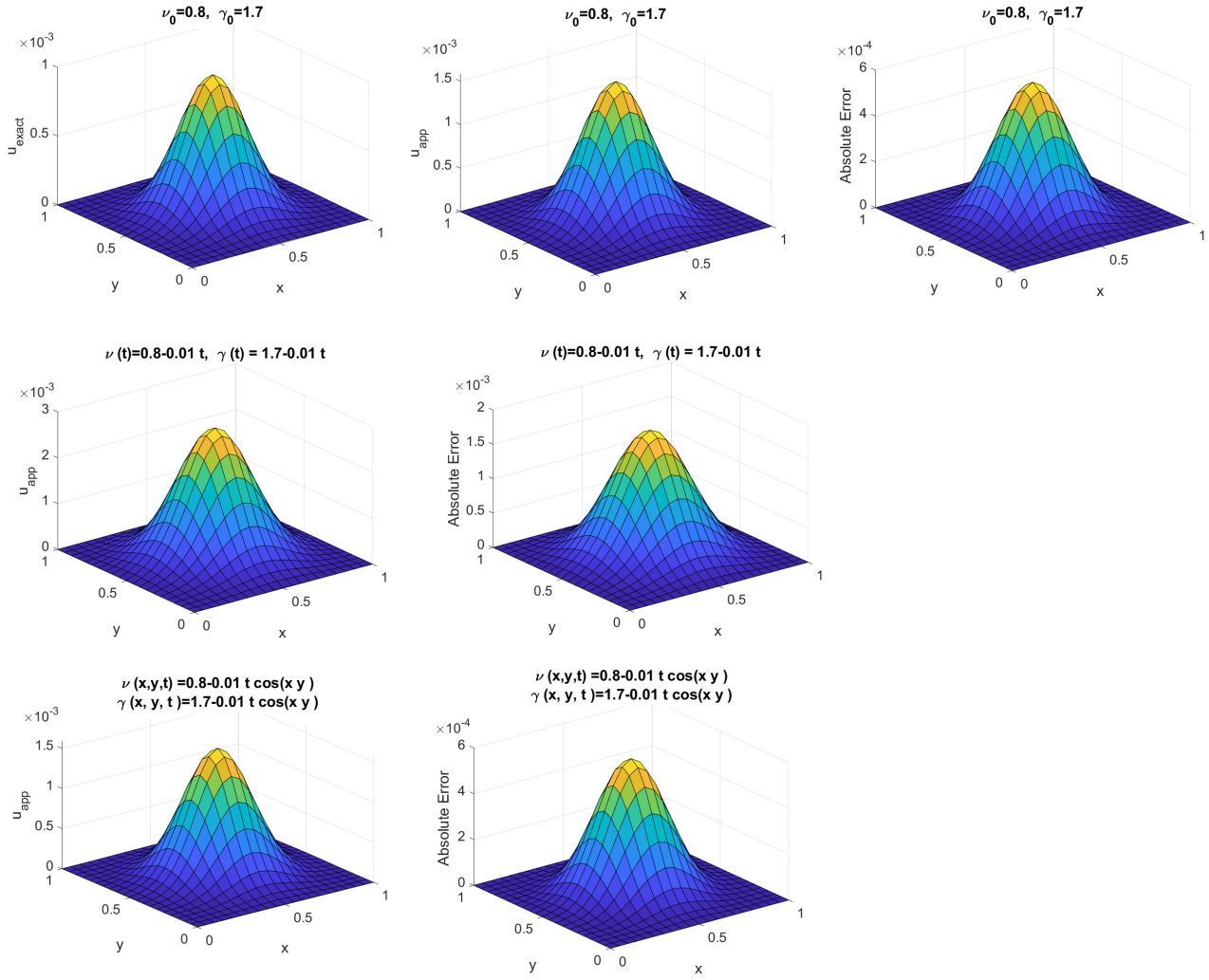

Figure 2. Comparing exact and approximate solution behavior in Problem 2 for $\ell = m = n = 20$, at different cases of ν, γ, and $(X, Y, T_f) = (1, 1, 0.1)$.

Problem 3

Consider the following 2-D VOFMDW as described in [1]:

$$f(x,t) = (3t^2 + 6t)(1 - x^2 - y^2) + 4(1 + t^3).$$

in which $t \in [0, T_f]$, and $\Omega \in [X_0, X] \times [Y_0, Y]$.

The initial conditions are:

$$u(x,y,0) = 0, \ \frac{\partial u(x,y,0)}{\partial t} = 0,$$

the corresponding boundary conditions are:

$$u(X_0,y,t) = (1+t^3)(1-X_0^2-y^2), \ u(X,y,t) = (1+t^3)(1-X^2-y^2),$$

$$u(x,Y_0,t) = (1+t^3)(1-x^2-Y_0^2), \ u(x,Y,t) = (1+t^3)(1-x^2-Y^2).$$

For these given conditions, the exact solution is: $u(x,y,t) = (1+t^3)(1-x^2-y^2)$.

Considering the step sizes $\tau(\triangle t) = p \sinh(\triangle t)$, $\kappa(\triangle x) = q \sinh(\triangle x)$ and $\kappa(\triangle y) = q \sinh(\triangle y)$ for which $q, p, \in (0,1)$. Figure **??** compares the exact and approximate solutions for u at β in (12) evaluated across the domain $(\Omega, t) \in [-0.2, 0.2]^2 \times [0, 0.2]$ for three distinct cases: (1) constant-order $\nu_0 = 0.8$, $\gamma_0 = 1.8$ (2) variable-order in linear

functions $\nu(t) = 0.8 - 0.01\,t$, $\gamma(t) = 1.8 - 0.01\,t$ and (3) variable-order in nonlinear functions $\nu(t) = 0.8 - 0.01\,e^t$, $\gamma(t) = 1.8 - 0.01\,e^t$. Table 4 presents the maximum error values of the WANSFDM for various values of (X, Y, T_f), using the discretization $\ell = m = n = 15$, with $X_0 = Y_0 = 0$, and at β as defined in Eq (12). The scheme is tested under three dominated cases of variable-orders $\nu(t)$ and $\gamma(t)$. As shown in the table, WANSFDM performs effectively across different types of variable-order scenarios, particularly in the wave-dominated case, demonstrating its accuracy and stability.

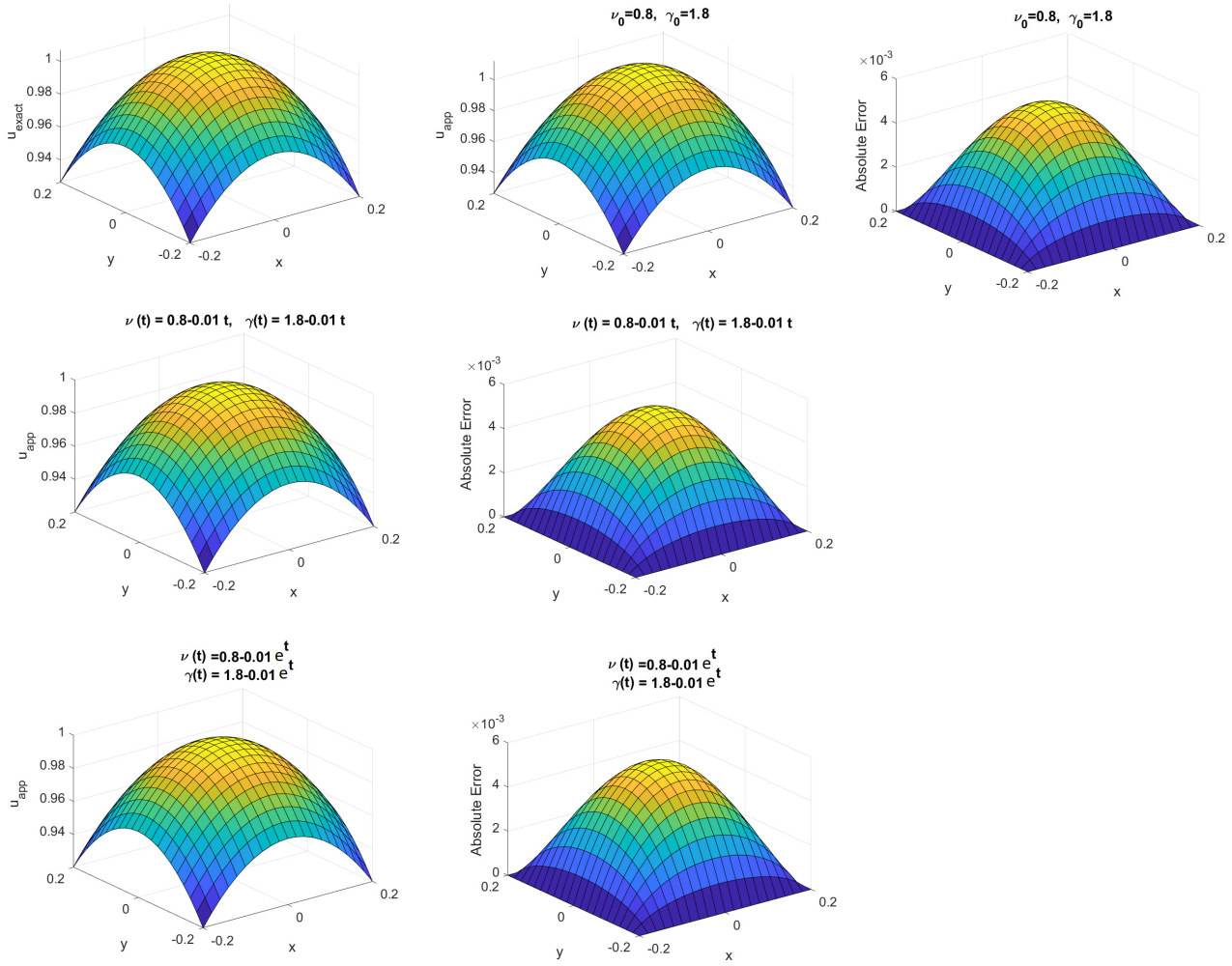

Figure 3. Comparing exact and approximate solution behavior in Problem 3 for $\ell = m = n = 20$, at different cases of ν, γ, and $(\Omega, t) \in [-0.2, 0.2]^2 \times [0, 0.2]$.

Table 4: The E_∞ error of WANSFDM at β in (12) for $\ell = m = n = 15$

(X, Y, T_f)	$\nu(t) = 0.9 - 0.01\,e^t$ $\gamma(t) = 1.3 - 0.01\,e^t$	$\nu(t) = 0.9 - 0.01\,e^t$ $\gamma(t) = 1.9 - 0.01\,e^t$	$\nu(t) = 0.3 - 0.01\,e^t$ $\gamma(t) = 1.8 - 0.01\,e^t$
(0.1,0.1,0.1)	3.607×10^{-4}	1.393×10^{-4}	2.063×10^{-4}
(0.1,0.1,0.2)	6.768×10^{-4}	2.178×10^{-4}	3.752×10^{-4}
(0.5,0.5,0.1)	4.991×10^{-3}	4.692×10^{-4}	9.778×10^{-4}
(1,1,1)	1.002×10^{-1}	4.372×10^{-2}	8.437×10^{-2}

5 Conclusion

This paper proposed and analyzed two weighted average finite difference schemes for solving the VOMDW model problem. By varying values of the weighting parameter β, the schemes were successfully applied to study the behavior of models in one and two spatial dimensions. A modified von Neumann stability analysis demonstrated the robustness of the proposed schemes, while truncation error analysis confirmed their second-order spatial accuracy $O(\Delta x^2 + \Delta y^2)$ and first-order temporal accuracy $O(\Delta t)$. The schemes maintained excellent stability across a wide range of variable-order cases and β values. The successful implementation of the WANSFDM confirms its effectiveness in approximating solutions. Furthermore, comparative results show that WANSFDM yields more accurate and stable solutions than WASFDM in dominated scenarios. The proposed WANSFDM provides a reliable and versatile numerical tool for modeling complex systems with evolving diffusive and wave-like behavior. All numerical simulations in this study implemented efficiently in MATLAB.

Acknowledgement

The authors are grateful to all anonymous reviewers for their valuable comments, which have provided great help for the improvement of the paper.

Funding This research received no specific grant from any funding agency in the public, commercial, or not-for-profit sectors.

References

[1] A.S. Alshehry, R. Shah, N.A. Shah, I. Dassios, A reliable technique for solving fractional partial differential equations, *Axioms* **11**(10), 574 (2022).
[2] V.E. Lynch, B.A. Carreras, D. del-Castillo-Negrete, K.M. Ferreira-Mejias, H.R. Hicks, Numerical methods for the solution of partial differential equations of fractional order, *Journal of Computational Physics* **192**, 406-421 (2003).
[3] K. Diethelm, N.J. Ford, Analysis of fractional differential equations, *Journal of Mathematical Analysis and Applications* **265**(2), 229-248 (2002). https://doi.org/10.1006/jmaa.2000.7194
[4] C. Li, F. Zeng, *Numerical Methods for Fractional Calculus*, Chapman & HallCRC, (2015).
[5] I. Podlubny, *Fractional Differential Equations*, Academic Press, San Diego, (1999).
[6] Z. Sun, C. Ji, D. Ruilian, A new analytical technique of the L-type difference schemes for time fractional mixed sub-diffusion and diffusion-wave equations, *Applied Mathematics Letters* **102**, 106115 (2020).
[7] A. Bhardwaj, A. Kumar, A numerical solution of time-fractional mixed diffusion and diffusion-wave equation by an RBF-based meshless method, *Springer* (2020).
[8] N.H. Sweilam, S.M. Ahmed, S.M. Al-Mekhlafi, Two-dimensional distributed order cable equation with non-singular kernel: a nonstandard implicit compact finite difference approach, *Applied Mathematics and Computational Mechanics* (2024).
[9] G.D. Smith, *Numerical Solution of Partial Differential Equations: Finite Difference Method*, 3rd ed., Oxford University Press, New York (1986).
[10] X. Zhao, Q. Xu, Efficient numerical schemes for fractional sub-diffusion equations with spatially variable coefficients, *Applied Mathematical Modelling* **38**, 3848-3859 (2014).
[11] K. Van Bockstal, Existence of a unique weak solution to a non-autonomous time-fractional diffusion equation with space-dependent variable order, *Advances in Difference Equations* **2021**, 1-43 (2021).
[12] H. Zhang, F. Liu, M.S. Phanikumar, M.M. Meerschaert, A novel numerical method for the time-variable fractional order mobile-immobile advection-dispersion model, *Computers & Mathematics with Applications* **65**(5), 693-701 (2013).
[13] S.G. Samko, B. Ross, Integration and differentiation to a variable fractional order, *Integral Transforms and Special Functions* **1**(4), 277-300 (1993).
[14] S.G. Samko, Fractional integration and differentiation of variable order, *Analysis Mathematica* **21**(3), 213-236 (1995).
[15] Y. Wang, L. Zhang, H. Li, Combination of discrete technique with Bernoulli polynomial approximation for solving a class of time distributed-order and space variable-order fractional damped diffusion-wave equation, *Applied Mathematics and Computation* (2025). https://doi.org/10.1007/s12190-024-02354-3
[16] D. Amilo, K. Sadri, E. Hincal, Comparative analysis of Caputo and variable-order fractional derivative algorithms across various applications, *International Journal of Applied and Computational Mathematics* **11**, 80 (2025). https://doi.org/10.1007/s40819-025-01887-w
[17] M. Khan, M. Khan, S. Sathasivam, High-order finite difference method for the two-dimensional variable-order fractional cable equation in complex systems and neuronal dynamics, *AIMS Mathematics* (2025).
[18] M. D. Ortigueira, D. Valério, J. Tenreiro Machado, Variable order fractional systems, *Communications in Nonlinear Science and Numerical Simulation* **71**, 231-243 (2019).

[19] S. Shen, F. Liu, V. Anh, I. Turner, J. Chen, A characteristic difference method for the variable-order fractional advection-diffusion equation, *Applied Mathematics and Computation* **219**(16), 1-16 (2013).
[20] H. Hassani, Z. Avazzadeh, J.A. Tenreiro Machado, Numerical approach for solving variable-order space-time fractional telegraph equation using transcendental Bernstein series, *Engineering Computations* (2019).
[21] J.E. Solis-Perez, J.F. Gomez-Aguilar, A. Atangana, Novel numerical method for solving variable-order fractional differential equations with power, exponential and Mittag-Leffler laws, *Chaos, Solitons & Fractals* **114**, 175-185 (2018).
[22] N.H. Sweilam, S.M. Al-Mekhlafi, Numerical study for multi-strain tuberculosis (TB) model of variable-order fractional derivatives, *Journal of Advanced Research* **7**(2), 271-283 (2016).
[23] C.F. Lorenzo, T.T. Hartley, Variable order and distributed order fractional operators, *Nonlinear Dynamics* **29**(1-4), 57-98 (2002).
[24] N.H. Sweilam, S.M. Al-Mekhlafi, S.A. Shatta, D. Baleanu, Numerical study for two types variable-order Burgers' equations with proportional delay, *Applied Numerical Mathematics* **156**, 364-376 (2020).
[25] N.H. Sweilam, M.M. Abou Hasan, Numerical solutions of a general coupled nonlinear system of parabolic and hyperbolic equations of thermoelasticity, *European Physical Journal Plus* **132**, 212 (2017).
[26] N.H. Sweilam, S.M. Al-Mekhlafi, A novel numerical method for solving 2-D time-fractional cable equation, *European Physical Journal Plus* **134**, 323 (2019).
[27] K.C. Patidar, Nonstandard finite difference methods: recent trends and further developments, *Applied Mathematics and Computation* **22**(6), 817-849 (2016).
[28] J. Wang, S. Yuan, X. Liu, Finite difference scheme and finite volume scheme for fractional Laplacian operator and some applications, *Fractals and Fractals* **7**(12), 868 (2023).